Available online at www.sciencedirect.com
SCIENCE DIRECT®
PERGAMON
International Journal of Heat and Mass Transfer 46 (2003) 4789–4797
International Journal of HEAT and MASS TRANSFER
www.elsevier.com/locate/ijhmt

A numerical simulation of pool boiling using CAS model

Jing Yang, Liejin Guo *, Ximin Zhang

State Key Laboratory of Multiphase Flow in Power Engineering (SKMFPE), Xi'an Jiaotong University, Xi'an 710049, China

Received 17 January 2003; received in revised form 8 June 2003

Abstract

This paper presents a new numerical model, called the CAS model, for boiling heat transfer. The CAS model is based on the cellular automata (CA) technique that is integrated into the popular SIMPLER algorithm for CFD problems. In the model, the CA technique deals with the microscopic nonlinear dynamic interactions of bubbles while the traditional CFD algorithm is used to determine macroscopic system parameters such as pressure and temperature. The popular SIMPLER algorithm is employed for the CFD treatment. The model is then employed to simulate a pool boiling process. The computational results show that the CAS model can reproduce most of the basic features of boiling and capture the fundamental characteristics of boiling phenomena. The heat transfer coefficient predicted by the CAS model is in excellent agreement with the experimental data and existing empirical correlations.

Keywords: Numerical simulation; Pool boiling; SIMPLER; Cell automata; CAS model

1. Introduction

Pool boiling is often encountered and widely used in the manufacturing, power and chemical industries because of its high efficiency of heat transfer. It is essential to have ability to predict accurately the rate of heat transfer in pool boiling under various pressures and geometry conditions so that one can design the heat transfer equipment with reduced cost, size or weight.

Great efforts have been devoted to measurements and modeling of boiling process in the past several decades. Forster and Zuber [1] presented the bubble agitation model in which the large heat transfer rates associated with nucleate boiling is considered as the consequence of the microconvection in the superheated sublayer caused by bubble agitation. The high thermal resistance of this sublayer is removed by the growth and collapse of vapor bubbles. Forster and Greif [2] proposed the vapor–liquid exchange mechanism, that is, the pulsating bubbles draw liquid from the bulk to the heating surface, then push the heated liquid back into the bulk and the bubble volume of hot liquid is transferred from the heating surface. Similarly, Han and Griffith [3] put forward the bulk convection theory, considered the departing bubbles bringing part of the layer of superheated liquid adjoining the bubble into the main body of fluid like a small pump. At the same time, the cold fluid flows on to the heating surface. By this kind of repeated bulk convection, heat is transferred from the heating surface to the main body of the fluid. The heating surface in pool boiling is divided into two parts, the bulk convection area and the natural convection area. Mikic and Rohsenow [4] revised the bulk convection theory by including the effect of heating surface characteristics, i.e. the cavity size distribution over the surface. Snyder [5] suggested a microlayer evaporation model in which heat is transferred by the evaporation of microlayer under growing vapor bubbles, as well as the condensation of vapor at the top of the bubbles where the vapor bubbles are contacted with relatively cold liquid. Jadd and Hwang [6] proposed a combined model in which the effects of bulk convection, natural convection and microlayer evaporation are integrated. Based on the combined model, Haider and Webb [7] took into account the effect of the departing bubble wake on the nucleate

* Corresponding author. Tel.: +86-29-266-3895; fax: +86-29-266-9033.
E-mail address: lj-guo@mail.xjtu.edu.cn (L. Guo).

0017-9310/$ - see front matter © 2003 Elsevier Ltd. All rights reserved.
doi:10.1016/S0017-9310(03)00353-3

Nomenclature

c_p	specific heat
g	gravity acceleration constant
h	enthalpy
h_{fg}	latent heat of evaporation
p	pressure
P	number defined in Eq. (6)
r	radius
R_a	surface roughness
S	source terms
t	time
T	absolute temperature
T_{sat}	saturation temperature
u	velocity along x coordinate
v	velocity along y coordinate
x	random number, defined in Eq. (6)

Greek symbols

ρ	density
σ	surface tension
μ	kinematic viscosity
κ	thermal conductivity

Subscripts

e	equilibrium
i	index number
ran	random number
cut	cut-off value

Superscripts

L	liquid
V	vapor

boiling heat transfer. The liquid rushing to the nucleation site in the wake of the departing bubble induces eddies. The superheated liquid in eddies would follow the bubble wake and would evaporate the liquid into the rising bubble. Zuber [8] analyzed nucleate pool boiling using an analogy with turbulent natural convection and expressed the nucleate boiling heat flux as a function of wall superheat and nucleation site density. Tien [9] presented a pool-boiling model based on the hydrodynamic similarity between the flow field associated with a rising bubble column and an inverted stagnation flow. Nevertheless, although some basic aspects have been involved in the existing models, there appears to be some discrepancies among these models and the physical mechanism of pool boiling is still not fully understood.

Various empirical or semi-empirical correlations based on the aforementioned models have been developed to calculate pool boiling heat transfer. These correlations can be classified into two types according to the method used to arrange them [10]. One kind of it is those regressed as dimensionless groups; these correlations are universal in some extent and used in a wider range because more parameters are included in it. While some variables included in this kind of correlations are really difficult to be determined or measured, such as departure diameter, departure frequency of vapor bubbles and nucleation site density, etc., so the application of these correlations are thus limited. Another kind of correlations is that composed of dimensional groups with simple and concise formula expression in which small amounts of variables are included. It is not universal enough to reflect the general heat transfer mechanism of pool boiling, because it is regressed from the experiment data of specified fluid under special environment, but it is more accurate in the specified application range. However, the majorities of the correlations available are somewhat empirical and can only be applied in relatively narrow ranges with considerable error bands.

Through the years, researchers are seeking for valid numerical methods to simulate the pool boiling process. Many models have been proposed and can be divided into two major categories: the deterministic models and probabilistic models. The deterministic models include the models using the traditional CFD methods (finite difference or finite element) to solve the conservation equations of mass, momentum, and energy, so as to determine the motion, interaction, and thermodynamic variations of the system. Once the governing equations, boundary and initial conditions are given, the results will be obtained in a deterministic way. For example, Spalding [11] proposed the IPSA (inter-phase-slip algorithm) numerical procedure for solving the equations of heat, mass and momentum transfer governing multiphase flow phenomena. The procedure operates on finite-difference equations connecting the values of variables pertain to points arrayed on a ''staggered'' topologically Cartesian grid. Lai and Farouk [12] applied the IPSA to the numerical simulation of boiling, while the details of the bubble dynamics and the characteristic properties of heating surface are ignored. Wang et al. [13] put forward a model that takes into account the time development of boiling phenomena in both micro- and macroscales. In microscale the model includes a detailed description of instantaneous local conduction, convection, energy and mass exchanges across the interfaces. The macroscopic descriptions of the model are then emerged as a natural consequence in a deterministic way by keeping track of the microscopic boiling dynamics. Similarly, He et al. [14] proposed a model based on the numerical macrolayer method. The boiling curves were reproduced

numerically by determining the macrolayer thickness. It postulated that vapor stems were formed on the active cavity sites with a certain contact angle and the evaporation occurs at the liquid–vapor interface. An initial spatial pattern of vapor stems was assumed and the experimental macrolayer thickness with wall superheat was employed. Subsequently, the heat flux was calculated according to the model and the simulated boiling curves were obtained. Wu et al. [15] suggested a method to simulate the bubble dynamics on the boiling surface by solving three-dimension transient conduction equation, and the bubble influence area, flow strength, wall temperature variation and bubble wait time are investigated. Son and Dhir [16,17] simulated the film boiling based on the Taylor instability theory. Lee and Nydahl [18] performed a numerical simulation of a single bubble based on the microlayer evaporation model.

The deterministic models discussed above are based on the solutions of the partial or differential equations of continuous system. The probabilistic models, on the other hand, deal with microscopic dynamics based on the evolving rules for temporal and spatial discrete systems. The complex behaviors of the whole system can be described by simple interactions of local regions in the probabilistic models, and the macroscopic physical characteristics can then be obtained by statistic average of microscopic variables. Many approaches have been tried to develop a probabilistic model. For example, Yang et al. [19] developed a model that is based on the lattice-Boltzmann method. The model describes the hydrodynamic aspects of bubble coalescence under nucleate boiling condition by simulating the growth and detachment behavior of multiple bubbles generated on the horizontal, vertical, and inclined downward-facing surfaces. Kimura and Maruyama [20,21], on the other hand, employed a molecular dynamics method to simulate the heterogeneous nucleation of liquid droplets on a solid surface. The spherical automata model [22] and the coupled map lattice method (CML) [23] have also been attempted for simulation of boiling.

In reality, boiling is a complex nonlinear dynamic process. Firstly, the microscopic aspects of boiling process, e.g. embryo nucleation and surface roughness, determine its nature largely, while the microscopic effects eventually exhibit in a macroscopic manner. Secondly, the boiling process seems to be stochastic without any rules to be abided by; no one can predict precisely where or when the next bubble will generate, vanish or coalesce. However, once the initial conditions and boundary conditions are given, the macroscopic boiling phenomenon emerges at the time as expected as if it has been planned in advance, in other word, boiling seems also to be deterministic. Thirdly, the boiling field is filled with a large amount of bubbles generated with the vapor–liquid interface kept on moving. As a whole, however, it is still a continuous system. Therefore, boiling is a process unifying the deterministic and stochastic, discrete and continuous, microscopic and macroscopic aspects. The existing models, either deterministic or probabilistic, are not able to capture the fundamental nature of the boiling process. The deterministic models neglect the random factors and phenomena occurred in microscopic level such as coalescence and vanishing of bubbles as well as the surface roughness effect of the heater. On the other hand, the probabilistic models have advantages over the traditional deterministic models in simulating random boiling phenomenon but it brings indelible statistic white noises to the macroscopic statistics.

This study proposes a new model, namely CAS model, for theoretical simulation of a boiling process. The CAS model integrates the nonlinear method—cellular automata (CA) [24]—with the traditional CFD method—SIMPLER (semi-implicit method for pressure linked equations revised) [25]. The paper presents a detailed description of the model. New experimental results are also presented to demonstrate the feasibility and effectiveness of the CAS model in simulating the boiling phenomena.

2. The CAS model

In pool boiling, a growing bubble causes the drop of the surface temperature adjacent to it. The bubbles also influence each other due to heat absorption or release as the neighbor vapor bubbles generate, grow and vanish. It's such continuous competition and cooperation that determines the boiling heat transfer. Such a nonlinear interaction is very difficult to be simulated by using a traditional, deterministic CFD method.

Here, the CA technique is introduced in the CAS model to simulate such nonlinear interactions among bubbles in a boiling process. The CA method alone, however, cannot completely describe the boiling process because of the existence of white noises coming from its statistical nature. Therefore, it is proposed here that the CA technique is incorporated into a traditional CFD algorithm, with the CA method dealing with the microscopic nonlinear dynamic interactions of bubbles while the traditional CFD algorithm is used to determine the macroscopic parameters, such as pressure, temperature. Patankar's SIMPLER method [25] is employed here for the CFD treatment.

CA deals with arrays of discrete cells with discrete values. The value at each cell evolves deterministically with time according to a set of definite rules involving the values of its nearest neighbors.

2.1. Cell and grid

In the present CAS model, the computational domain is divided into regular hexagon cell lattice of equal

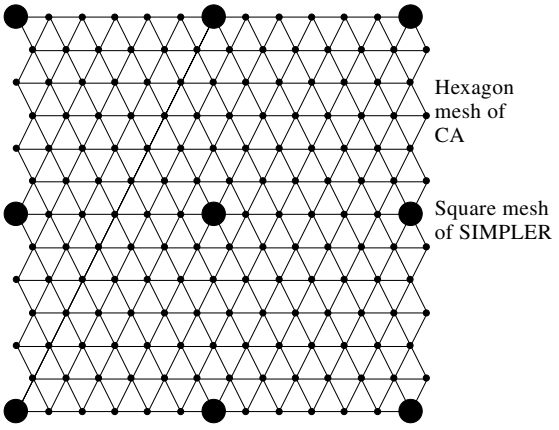

Fig. 1. Two superposed grid schemes used in the CAS model: a hexagon mesh for CA and a square mesh for SIMPLER algorithm.

size (in two-dimensions), and a SIMPLER square mesh is then superimposed to the CA network as shown in Fig. 1. The regular mesh of the hexagon cells with a much finer scale is used for modeling of vapor bubble formation with the CA technique. Each cell is characterized by different variables (e.g., temperature, pressure) and states (liquid or vapor). The aim of this combination is to predict simultaneously the microstructure development as a function of the thermal field and the influence of the latent heat release of the cells on the calculated thermal history.

2.2. Governing equations

Though boiling phenomena is complicated, the thermal convection and diffusion are still governed by the equations of motion (Navier–Stokes equations) and the equation of energy conservation.
Mass conservation equation:

$$\frac{\partial \rho}{\partial t}+\frac{\partial(\rho u)}{\partial x}+\frac{\partial(\rho v)}{\partial y}=0. \tag{1}$$

Momentum conservation equation-x:

$$\frac{\partial(\rho u^2)}{\partial x}+\frac{\partial(\rho uv)}{\partial y}=-\frac{\partial p}{\partial x}+\frac{\partial}{\partial x}\left(\mu\frac{\partial u}{\partial x}\right)+\frac{\partial}{\partial y}\left(\mu\frac{\partial u}{\partial y}\right). \tag{2}$$

Momentum conservation equation-y:

$$\frac{\partial(\rho uv)}{\partial x}+\frac{\partial(\rho v^2)}{\partial y}=-\frac{\partial p}{\partial y}+\frac{\partial}{\partial x}\left(\mu\frac{\partial v}{\partial x}\right)+\frac{\partial}{\partial y}\left(\mu\frac{\partial v}{\partial y}\right)-g\rho. \tag{3}$$

Energy conservation equation:

$$\frac{\partial(\rho uh)}{\partial x}+\frac{\partial(\rho vh)}{\partial y}=\frac{\partial}{\partial x}\left(\kappa\frac{\partial T}{\partial x}\right)+\frac{\partial}{\partial y}\left(\kappa\frac{\partial T}{\partial y}\right)+S. \tag{4}$$

The meanings of symbols are defined in the nomenclature.

Although two phase mixture, i.e., vapor + liquid, are involved in the boiling process, the phase-conservation equations of components (vapor and liquid) are excluded in the CAS model because the phase transition is considered in the scale of CA, and the effect of it is counted in by the coupling of CA and SIMPLER described in the following section. For such a complex phenomena as boiling, it is much more important to capture the fundamental nature, even though it is qualitative, rather than the strict and detailed calculation.

2.3. Treatment of bubble nucleation

During nucleate boiling, steam bubbles are generated from specific site, such as cavities or scratches on the surface that can trap vapor. The total number of active sites available depends on the surface condition, material and the heat flux level. In the CAS model, bubble nucleation is randomly initiated on the surface after the cell temperature satisfies the following discriminant for nucleation [26]:

$$T^{\mathrm{L}}-T_{\mathrm{sat}}>\frac{2\sigma T_{\mathrm{sat}}}{\rho^{\mathrm{V}}h_{\mathrm{fg}}r_{\mathrm{e}}}, \tag{5}$$

where T^{L} is the liquid temperature, T_{sat} is the saturation temperature, σ is the surface tension, ρ^{V} is the density of vapor, h_{fg} is the latent heat, and r_{e} is the critical radius of bubble nucleus.

Bubble nucleation in boiling is treated as a random process in the CAS model through a random number, x_{ran} which is generated following the Poisson distribution function [27] as follows:

$$P(R_{\mathrm{a}},x_{\mathrm{ran}})=\frac{\mathrm{e}^{-f(R_{\mathrm{a}})}f(R_{\mathrm{a}})^{x_{\mathrm{ran}}}}{(x_{\mathrm{ran}})!}, \tag{6}$$

where R_{a} is the arithmetic roughness of the surface. The expression $f(R_{\mathrm{a}})$ in Eq. (6) is determined by the material of heater surface and the liquid. The exponent $f(R_{\mathrm{a}})$ is simply assigned as a constant in our calculation, however, written as a function here for the sake of compatibility so as to extend the CAS model to the other situations in the future. For each cell on the surface and any given x_{ran} and R_{a}, Eq. (6) can give a number P. Once P is larger than a prescribed cut-off value P_{cut}, this surface cell (or cite) is then nucleated with vapor bubble. The cell then converts to active nucleus from which steam bubble grows.

2.4. Rules of cell evolution

In the CAS model, the cells of CA have values of either zero or one. At each time step, all of the sites of

the domain are simultaneously updated by applying rules to the neighborhoods of each site. The rules of cell evolution are defined as follows:

- Any cell with its three nearest neighbor cells vaporized stays vaporized.
- A vaporized cell with two nearest neighbor cells vaporized remains vaporized.
- All other cells remain as a liquid state.
- During the growth of a vapor bubble, the cells that were caught by the growing bubble become active nucleuses.
- When a growing cell has all of its neighbors with a nonzero index number, it will no longer grow.

2.5. Coupling of the CA model with the SIMPLER algorithm

The coupling of the CA with the SIMPLER algorithm is realized through the energy conservation equation, Eq. (4). It is known that the enthalpy variation of a control volume in a boiling process consists of two parts: one is caused by the variation of temperature (sensible heat); another is caused by the phase transition (latent heat). Therefore, the variation in the enthalpy of any given node n (δh_n) can be calculated based on the temperature variation (δT_n) of the node and the variation of the void fraction (δv_n) of the node:

$$\delta h_n = \rho c_p \delta T_n - h_{\mathrm{fg}} \delta v_n = \rho c_p \left[T_n^{t+\delta t} - T_n^t \right] - h_{\mathrm{fg}} \delta v_n. \tag{7}$$

The variation of the nodal temperature and enthalpy are obtained by solving the energy conservation equation together with all other governing equations based on the SIMPLER algorithm. The temperature at each cell is then determined by linear interpolation using the nodal temperatures obtained. For example, the temperature of the cell i at time t, T_i^t, can be obtained by the linear interpolation from the temperatures of the four nodal points of the SIMPLER square meshes around, T_n^t:

$$T_i^t = \sum_n c_{i,n} \cdot T_n^t, \tag{8}$$

where $c_{i,n}$ are the interpolation coefficients.

The state of each cell is determined by the method described in Section 2.3 and evolves according to the rules listed in Section 2.4. When the state of a cell varies from liquid to vapor, the void fraction variation at this cell is expressed as δv_i. The void fraction variation of the associated nodal point n, δv_n, is then calculated by that of all the cells associated with it:

$$\delta v_n = \frac{\sum_i c_{i,n} \delta v_i}{\sum_i c_{i,n}}, \tag{9}$$

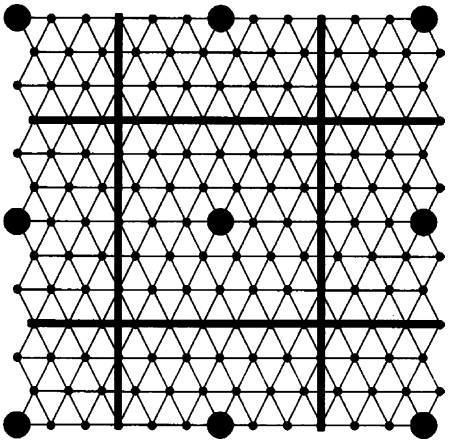

Fig. 2. SIMPLER node is associated with the cells included in the thick lines around the node.

where the SIMPLER node is associated with the cells included in the thick lines around the node (Fig. 2). Once δv_n is determined, the nodal temperature can then be updated based on Eq. (7):

$$T_n^{t+\delta t} = \frac{\delta h_n + h_{\mathrm{fg}} \delta v_n}{\rho c_p} + T_n^t. \tag{10}$$

2.6. Calculation procedure

Fig. 3 shows the flow chart of the CAS model. At the beginning of the simulation, each cell is given the same initial temperature below the liquid, and assigned a state index equal to zero. The sites located immediately next to the wall have a reference number that indicates they belong to this boundary. The time-matching calculation is then started. Periodic boundary condition is assumed at both sides of the boiling field. Therefore, the cells on the right boundary have their east neighbor located on the left boundary and vice versa.

3. Experimental setup

3.1. Description

The experimental device is composed of four main parts: the boiling vessel, the condensation system, data acquisition system and power supply system, as shown in Fig. 4. The condensation system is connected with the boiling vessel so as to keep the pressure in the boiling vessel constantly. The condensed liquid is returned back to the boiling vessel through a tube connected on the low part of it. An U-type manometer is used to monitor the pressure of working medium in the boiling vessel, meanwhile also served as a security valve in the case that

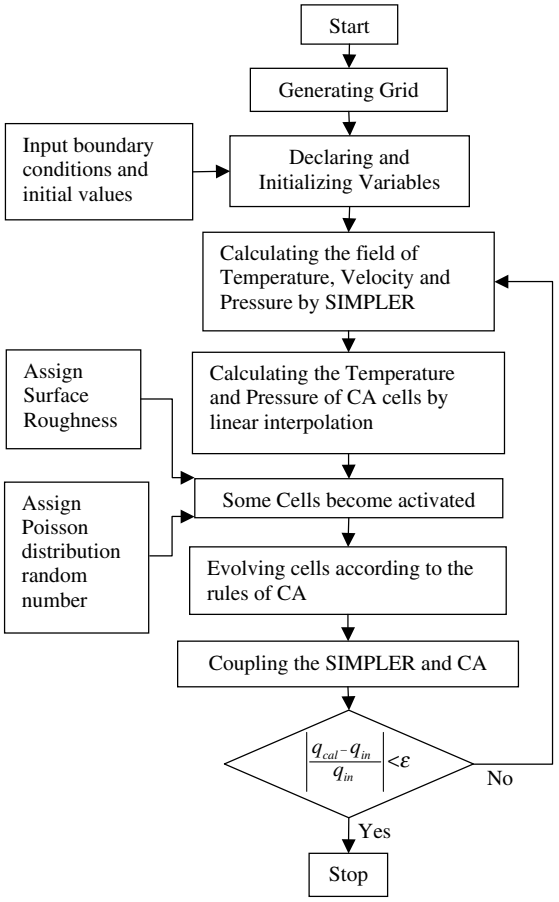

Fig. 3. Flow chart of the CAS model.

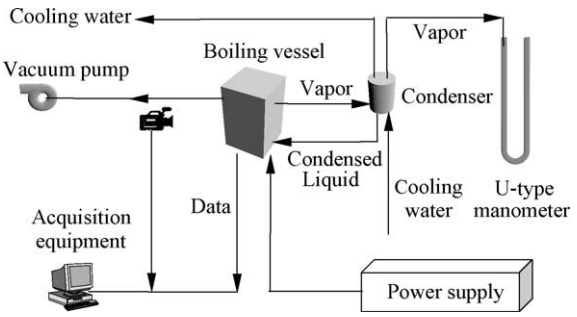

Fig. 4. Experimental setup composed of the boiling vessel, the condensation devices, the acquisition system and the power supply system.

the pressure in the boiling vessel is too high for accident and will release the pressure immediately. The accuracy of the pressure is about 10 Pa. The visualization of the boiling process through the transparent view windows of the boiling vessel is recorded by a Sony CCD-TRV318 camcorder.

3.2. Boiling vessel

The boiling vessel is made of stainless steel with 110×110 mm^2 cross-section and 130 mm height as shown in Fig. 5. A plate heater is located at the bottom of the boiling vessel. The plate heater is made of a quartz glass plate with 20×60 mm^2 area (4 mm in thickness) and exposed to the test liquid directly. On the surface opposite to the heat transfer side, a transparent ITO film is coated and operated as heater by applying electric current through it. The power input is determined from the measured electric voltage and current imposed on the heater. The accuracy of voltage measurement is 0.1 V, the accuracy of current measurement is 0.025 A. In addition, there is two auxiliary heaters are installed beside the plate heater for supplying heat prior to the plate heater. There is a pair of view windows with the vacuum interlayer in the front and rear face of boiling vessel. The interlayer is evacuated by the vacuum pump to the pressure below 0.06 Pa during the experiment. A three-dimension coordinate frame is set on the top of the boiling vessel for determining the coordinate of the point being detected during boiling. The accuracy of the coordinate measurement is 0.01 mm. The whole boiling vessel is insulated by a thick layer of Polyurethane foam for heat preservation. The energy balance to the evidence heat loss of the boiling vessel is under 3%.

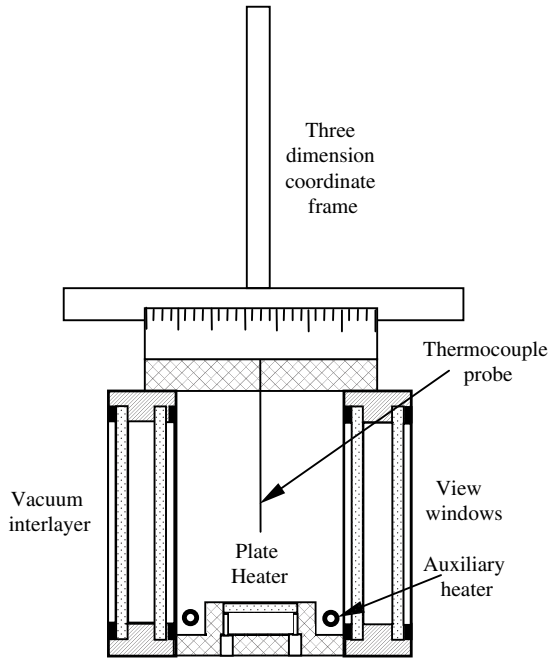

Fig. 5. Schematic of the boiling vessel.

3.3. Temperature instrumentation

On the heat transfer side of the plate heater, some thin copper and constantan electrodes of 0.2 μm thicknesses were coated directly on the glass substrate as shown in Fig. 6. Two electrodes were made contact at the end of each as the hot conjunction to form a thermocouple of T-type for temperature measurement of heater surface. Total nine thermocouples were employed on the heater surface. In addition, a T-type thermocouple probe (shown in Fig. 5) with a diameter of 0.5 mm is fixed on the three-dimension coordinate frame for detecting the temperature of fluid in the boiling vessel. The accuracy of the temperature measurements is 0.3 °C. The data acquisition is carried out by a Schlumberger SI 35951C IMP with 20 Hz acquisition frequency.

3.4. Experimental procedure

At the beginning of the experiment, the vacuum interlayer of the boiling vessel was evacuated firstly by the vacuum pump and the vessel was filled with testing liquid; then the two auxiliary heaters were turned on to bring the fluid in the boiling vessel to the saturation temperature and to drive off dissolved gases. In order to avoid large thermal stress emerged in the quartz glass plate heater due to temperature rising it was heated slowly. When the fluid temperature reached the saturate temperature, the two auxiliary heaters were turned off, and the plate heater was turned on. The fluid was kept boiled for a few hours to achieve a steady state condition. In the mean time, the system pressure was maintained constant at 1 atm by the condenser connected with the boiling chamber. For a fixed heat flux, the temperature, voltage and current measurements, as well as the visualization of the boiling process, were taken into computer by acquisition system. The heating power was stepped up; then the new state was established and investigated. This procedure was repeated until the acceptable maximum heat flux of the heater was reached.

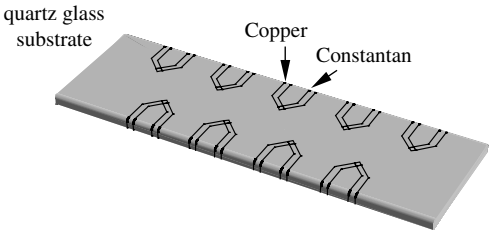

Fig. 6. Schematic of the heater (on the back) and the thermocouple distribution.

4. Result and discussion

This CAS model was employed to predict pool boiling of water under various conditions in the present work. The results of model prediction were compared with available experimental data. The initial temperature of water ranges from 30 to 100 °C, i.e., from a subcooled to a saturated condition. A two-dimensional square was chosen as the boiling field of calculation for the convenience. The bottom of the square was heated with a constant heat flux and the temperature at the top of the field was fixed at a constant prescribed temperature. A periodic boundary condition was applied to both sides of the boiling field.

4.1. Boiling curve

Fig. 7 shows a comparison of the boiling curve predicted by the CAS model (solid line) with the experimental data. For comparison, the predictions from the two empirical correlations proposed by Михеев [28] and Rohsenow [29], are also included in Fig. 7. It is found that both the empirical correlations of Михеев and Rohsenow overestimate the heat flux in the high superheat region, and the prediction made by the empirical correlation of Михеев is much higher than that of Rohsenow. However, the CAS model prediction is in an excellent agreement with the experimental data, in particular in the high superheat region. In the low superheat region, the CAS model a little underestimates the heat flux. A good agreement between the model and the data in the high superheat region indicates that the present CAS model captures the fundamental nature of boiling when vapor bubbles are abundantly generated and frequently interacted. On the other hand, it can be drawn from the comparison result that the considerable prediction error bands made by the empirical correlations in the high superheat region are because the

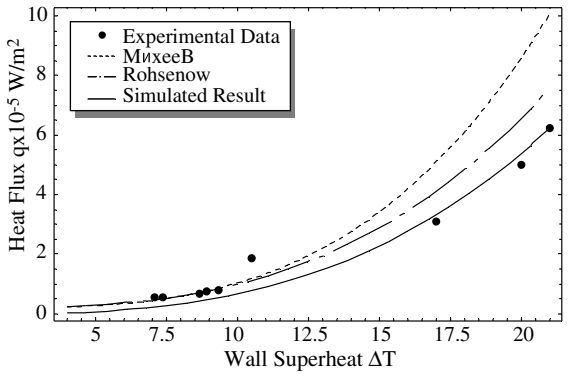

Fig. 7. Comparison of the CAS model prediction with experimental data and the empirical correlations.

interactions between vapor bubbles are not considered in the traditional predicting methods, but it is considered in the CAS model.

4.2. Snapshots of the boiling pattern

The snapshots of boiling pattern are given in Fig. 8. The state of boiling is changing continuously according to the evolving rules of the CAS model at each time step. Each state is recorded as a frame of a "video". Herein, only two snapshots of them are chosen arbitrarily for demonstration purpose. By playing these frames one after another, one can visualize the entire boiling process with major boiling modes, including nucleation, growth, coalescence and condensation of vapor bubbles.

From the results of the CAS model, it can be found that there exist some drawback needs to be improved, although the CAS model exhibits some advantage and have achieved some success in simulating the boiling phenomena. There are some aspects that are not consistent with the physical reality, e.g. some vapor bubbles are in shape of rectangle, which will never occur in nature, sometimes, the liquid is contained in the vapor bubble. Perhaps it is because of the irrationality of the rules of cell evolution that should be derived strictly from the control equations of the boiling process; however, the cell evolution rules are assigned subjectively from the physical natures of the boiling phenomena herein. In addition, the volume change caused by the density change is not considered in the CAS model; otherwise, it will be too complex to be solved.

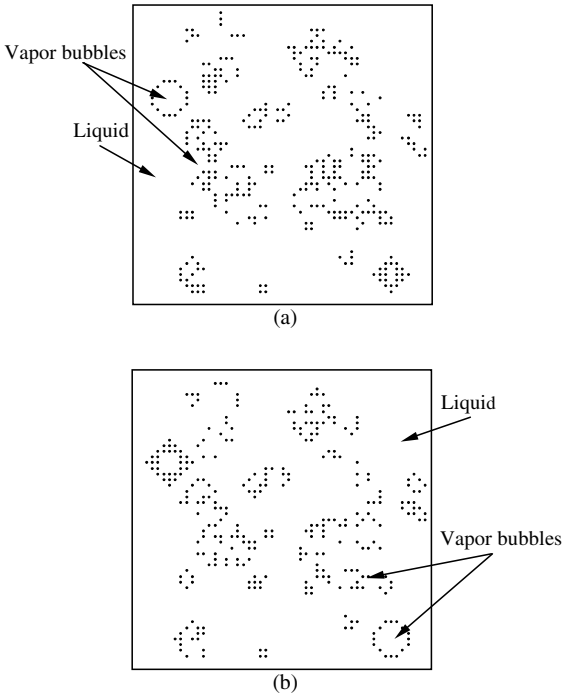

Fig. 8. Two snapshots of the pool boiling pattern.

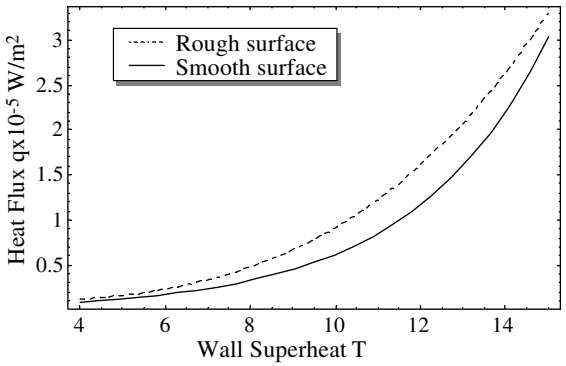

Fig. 9. Predicted boiling curves for two surfaces with different surface roughness.

4.3. Effect of the surface roughness

Fig. 9 shows the predicted boiling curves for two surface conditions: a rough surface ($R_a = 14.27$) and a smooth surface ($R_a = 9.38$). As one can see, the rough surface produces a higher heat flux than that of a smooth surface due to increased surface active sites. The present CAS model is able to reproduce the roughness effect, at least in a qualitative way.

5. Conclusion

The paper presents a new model for pool boiling. The model integrates the CA method into a traditional CFD algorithm. Computational experiments demonstrate that the CAS model is able to capture the essential physics underlying pool boiling and its prediction agrees well with our own experimental data as well as the empirical correlations available in the literature.

The study demonstrates that the CA technique is compatible with the traditional CFD method. Since the CAS model can be considered as an approach coupling microscopic molecular dynamics and conventional macroscopic fluid dynamics, it should be also applicable in the cases where the microscopic statistics and macroscopic description of a system are all considerably important, e.g., the multiphase multicomponent systems involving surface tension, capillarity and phase transition.

Acknowledgements

The financial supports by the National Natural Science Foundation of China (grant no. 59995462 and no. 10172069) are gratefully acknowledged.

References

[1] H.K. Forster, N. Zuber, Dynamics of vapor bubbles and boiling heat transfer, AIChE J. 1 (4) (1955) 531–535.

[2] K.E. Forster, R. Greif, Heat transfer to a boiling liquid-mechanism and correlations, J. Heat Transfer (February) (1959) 43–53.

[3] C.Y. Han, P. Griefith, The mechanism of heat transfer in nucleate pool boiling, Int. J. Heat Mass Transfer 8 (1965) 887–914.

[4] B.B. Mikic, W.M. Rohsenow, A new correlation of pool boiling data including the effect of heating surface characteristics, J. Heat Transfer, Trans. ASME (May) (1969) 245–250.

[5] N.W. Snyder, Summary of conference on bubble dynamics and boiling heat transfer, JPL momo 20-137 Cali. Inst. Technology, 1956.

[6] A.L. Jadd, K.S. Hwang, A comprehensive model for nucleate pool boiling heat transfer including microlayer evaporation, J. Heat Transfer 98 (1976) 623–630.

[7] S.I. Haider, R. Webb, A transient micro-convection model of nucleate pool boiling, Int. J. Heat Mass Transfer 40 (15) (1997) 3675–3688.

[8] N. Zuber, Nucleate boiling. The region of isolated bubbles and the similarity with natural convection, Int. J. Heat Mass Transfer 6 (1963) 53–78.

[9] C.L. Tien, A hydrodynamic model for nucleate pool boiling, Int. J. Heat Mass Transfer 5 (1962) 533–540.

[10] R.T. Lin, Boiling heat transfer, Scientific Press, China, 1988, pp. 154–163.

[11] D.B. Spalding, Numerical computation of multi-phase fluid flow and heat transfer, EPRI WS-78-143, vol. 2, 1980, pp. 139–167.

[12] J.C. Lai, B. Farouk, Numerical simulation of subcooled boiling and heat transfer in vertical ducts, Int. J. Heat Mass Transfer 36 (6) (1993) 1541–1551.

[13] S.S. Wang, R.E. Ferguson, J.H. Stuhmiller, A numerical method for steam-water two-phase flow heat transfer simulation, in: Numerical Properties and Methodologies in Heat Transfer, Proceedings of the 2nd National Symposium, College Park, MD, USA, 1983, pp. 437–460.

[14] Y. He, M. Shoji, S. Maruyama, Numerical study of high heat flux pool boiling heat transfer, Int. J. Heat Mass Transfer 44 (2001) 2357–2373.

[15] Y. Wu, C. Yang, X. Yuan, Numerical simulation of heat transfer in nucleate pool boiling, Huagong Xuebao/J. Chem. Ind. Eng. (China) 53 (5) (2002) 479–486.

[16] G. Son, V.K. Dhir, Numerical simulation of film boiling near critical pressures with a level set method, J. Heat Transfer, Trans. ASME 120 (1) (1998) 183–192.

[17] G. Son, V.K. Dhir, Numerical simulation of saturated film boiling on a horizontal surface, J. Heat Transfer, Trans. ASME 119 (3) (1997) 525–533.

[18] R.C. Lee, J.E. Nydahl, Numerical calculation of bubble growth in nucleate boiling from inception through departure, J. Heat Transfer, Trans. ASME 111 (2) (1989) 474–479.

[19] Z.L. Yang, T.N. Dinh, R.R. Nourgaliev, R.R. Sehgal, Numerical investigation of bubble coalescence characteristics under nucleate boiling condition by a lattice-Boltzmann model, Int. J. Thermal Sci. 39 (2000) 1–17.

[20] T. Kimura, S. Maruyama, A molecular dynamics simulation of heterogeneous nucleation of liquid droplet on a solid surface, Microscale Thermophys. Eng. 6 (2002) 3–13.

[21] S. Maruyama, T. Kimura, A molecular dynamics simulation of a bubble nucleation on solid surface, Int. J. Heat Technol. 18 (2000) 69–74.

[22] V. Herrero, G. Guido-Lavalle, A. Clausse, Simulation of boiling environments using geometrical automata, in: Proceedings of the First International Conference on Heat Transfer, Fluid Mechanics, and Thermodynamics, Kruger Park, South Africa, 2002.

[23] M. Shoji, Boiling simulator—a simple theoretical model of boiling, in: Proceedings of the Third International Conference on Multiphase Flow, Lyon, France, 1998.

[24] S. Wolfram, Universality and complexity in cellular automata, Physica D 10 (1984) 1–35.

[25] S.V. Patankar, Numerical Heat Transfer and Fluid Flow, Scientific Press, China, 1984, pp. 12–120 (Chinese translation by Z. Zhang).

[26] M.D. Xin, Boiling Heat Transfer and Its Enhancement, Chongqing University Press, China, 1987, pp. 7–35.

[27] M. Sultan, R.L. Judd, Spatial distribution of active sites and bubble flux density, J. Heat Transfer, Trans. ASME 100 (1) (1978) 56–62.

[28] М.А. Михеев, Основы теплопередачи, государственное энергетическое издатеьство, 1949, pp. 136–140.

[29] W.M. Rohsenow, J.P. Hartnett, E.N. Ganic, Handbook of Heat Transfer Fundamentals, second ed., McGraw-Hill, New York, 1985, pp. 12.2–12.8.